



ELSEVIER

Journal of Nuclear Materials 283–287 (2000) 446–450

Journal of  
nuclear  
materials

www.elsevier.nl/locate/jnucmat

# The effects of irradiation and testing temperature on tensile behaviour of stainless steels

C. Bailat<sup>a,\*</sup>, A. Almazouzi<sup>a</sup>, N. Baluc<sup>a</sup>, R. Schäublin<sup>a</sup>, F. Gröschel<sup>a,b</sup>,  
M. Victoria<sup>a</sup>

<sup>a</sup> EURATOM Association, Swiss Confederation, Ecole Polytechnique Fédérale de Lausanne, CRPP, Fusion Technology,  
Materials Group, 5232 Villigen PSI, Switzerland

<sup>b</sup> Labor für Werkstoff Verhalten, 5232 Villigen PSI, Switzerland

## Abstract

Irradiated 304 and 316 stainless steel samples were investigated. The steels were neutron irradiated to 1.5 and 7.5 dpa at 550 K. Similar types of steels were irradiated at 550 K with 590 MeV protons in the PIREX facility at PSI, Switzerland. The doses reached in this case were 0.15 and 0.3 dpa. The stress–strain relationships at different temperatures were measured. The irradiation and deformation microstructures were investigated using transmission electron microscopy (TEM). Two modes of deformation were found, twinning and channelling, depending on the testing temperature. These results are discussed in terms of deformation mechanisms at different temperatures correlated with radiation hardening. Finally, possible correlations between deformation modes and previous irradiation assisted stress corrosion cracking (IASCC) studies are discussed. © 2000 Elsevier Science B.V. All rights reserved.

## 1. Introduction

There are two motivations behind the present research. First, it is part of an investigation on the issue of the contribution of radiation hardening to the irradiation assisted stress corrosion cracking (IASCC) phenomena. Secondly and derived from the first, there is an insufficient amount of data available in the literature in the region of operating conditions of light water reactors (LWR) and fusion reactors utilising austenitic stainless steel.

The existence of a threshold fluence ( $\sim 10^{20}$  n/cm<sup>2</sup>) for IASCC susceptibility, found after irradiation, indicates that while in situ effects (corrosion potential, conductivity, temperature) are important, only persistent radiation effects (microstructural and microchemical

changes) can be responsible for the behaviour in post-irradiation tests [1].

The fundamental knowledge of radiation-induced processes controlling cracking resistance of austenitic stainless steels has been improved over the last ten years. Many aspects can be better explained, as for example the change in mechanical properties. However, the specific microstructural and microchemical components which promote cracking remain unknown [1]. An investigation of austenitic stainless steels commonly used in reactor engineering and a better understanding should help to optimise the safety of reactors. Furthermore, it will increase the lifetime of any component in irradiating environment [2].

It is thought that the intrinsic deformation mode found in pure fcc irradiated materials in this temperature region, namely dislocation channelling, could lead to instabilities at grain boundaries, because of the large localised shear strains implied. The possibility of testing the same stainless steel specimens that have been investigated by ABB Sweden in corrosion studies, provide a link to IASCC and the means of eventual correlation.

\* Corresponding author. Tel.: +41-56 310 4707; fax: +41-56 310 4529.

E-mail address: bailat@psi.ch (C. Bailat).

The present work attempts then to describe and correlate the radiation hardening, irradiation microstructure and deformation modes.

## 2. Experimental procedures

### 2.1. Material

The primary stainless steels used in reactor components are of type 304 and 316. Four different grades of stainless steel were supplied by ABB. They consisted of two grades of SS304L and SS316L, designated high purity (HP) and commercial purity (CP), respectively (see [3] for the detailed compositions). Tensile test results of the unirradiated and irradiated specimens show no systematic effects of the impurities [3]. Therefore, we will limit our comparisons between SS304 and SS316, neglecting the effect of impurity.

### 2.2. Irradiation

The steels were irradiated with either neutrons or high-energy protons. The neutron irradiations were performed in the Swedish light water reactor power plant Barsebäck 1. Two sets of samples were delivered by ABB: the first set reached a dose of 1.5 dpa and the second 7.5 dpa. The proton irradiations were performed at 520 K in the PIREX facility at PSI [4] in order to complete the test matrix with low dose irradiations. The doses achieved are 0.15 and 0.3 dpa.

The comparison of the two types of irradiation must be done carefully, as the high-energy protons used for simulation of fission neutrons produce impurities, particularly helium and hydrogen. However, the influence on the mechanical properties should be negligible at low doses. Previous studies performed on pure materials have shown that, at the doses used in the present study, a comparison between the defect microstructure and tensile properties produced by neutrons or high-energy protons based on displacement damage (dpa) shows no differences [5].

## 3. Results and discussion

### 3.1. Irradiation defect microstructure

The irradiation defect microstructure is an important parameter in understanding the behaviour of irradiated materials. Irradiated undeformed samples were systematically investigated and the defect sizes and densities were obtained using transmission electron microscopy (TEM). The results are summarised in Table 1. The mean loop size at 0.15 dpa is about 2.5 nm and with increasing dose, the mean loop size increases to approximately 8 nm. SS316L shows systematically smaller loop sizes than SS304L.

The loop density is between  $1.2 \times 10^{23} \text{ m}^{-3}$  at 0.15 dpa and  $3 \times 10^{23} \text{ m}^{-3}$  at 7.5 dpa for SS304L; SS316L shows systematically smaller densities, between  $1.7 \times 10^{22}$  and  $1.8 \times 10^{23} \text{ m}^{-3}$ . The density increases with dose and this increase is larger for SS316L than SS304L. The mean defect size increases with dose. Although larger loops could be observed, a distribution of small Frank type loops are superimposed at high doses.

### 3.2. Radiation hardening

The first issue is the effect of irradiation on the mechanical properties of the different samples.

Tensile tests were performed at room temperature and at 550 K, with unirradiated specimens and samples irradiated to different doses. A strain rate of  $1.5 \times 10^{-4} \text{ s}^{-1}$  was set for all tests. The yield strength was measured at 0.2% and the uncertainties on the values obtained are below 10% [1].

Due to the very high residual radioactivity of the high doses samples, mechanical testing was not possible on all samples at this stage. Therefore, in order to complete the test matrix, microhardness tests were performed on irradiated and unirradiated polished specimens. Using the yield strength values obtained from tensile tests of less radioactive samples, the microhardness was found approximately proportional to 2/3 of the yield strength. Furthermore, the increase in microhardness is known to

Table 1

Defect density and mean loop size for high and commercial purity SS304L and SS316L, irradiated to doses of 0.15, 1.5 and 7.5 dpa

Specimen	Dose	Density of black dots ( $\text{m}^{-3}$ )	Density of loops ( $\text{m}^{-3}$ )	Mean loop size (nm)
SS304L CP	p <sup>+</sup> -irr. 0.15 dpa	$1.7 \times 10^{23}$	$1.2 \times 10^{23}$	3.1
	n-irr. 7.5 dpa	–	$3 \times 10^{23}$	7.3
SS304L HP	n-irr. 1.5 dpa	–	$1.6 \times 10^{23}$	7.5
SS316L CP	p <sup>+</sup> -irr. 0.15 dpa	$1.6 \times 10^{22}$	$1.7 \times 10^{22}$	2.3
	n-irr. 7.5 dpa	–	$1.7 \times 10^{23}$	5.9
SS316L HP	n-irr. 1.5 dpa	–	$6.8 \times 10^{22}$	6.5
	n-irr. 7.5 dpa	–	$1.8 \times 10^{23}$	6.5

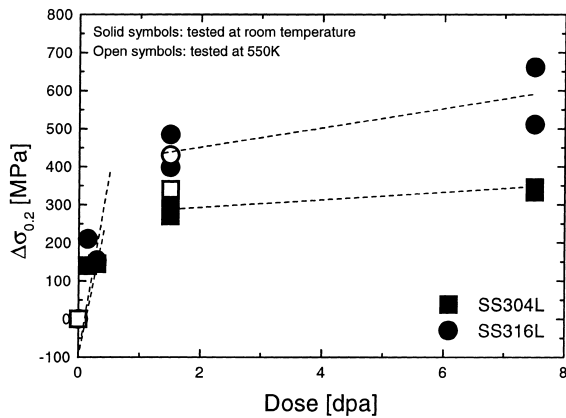


Fig. 1. Increase in yield strength as a function of dose at room temperature (solid symbol) and 550 K (empty symbol).

be directly proportional to the increase in yield strength [6].

Using the tensile test and microhardness results, the increase in yield strength as a function of dose at room temperature and at 550 K can be calculated. The results are shown in Fig. 1.

The hardening can be regarded as the increase in yield strength. At room temperature, the hardening at low doses increases rapidly and linearly with dose, while that produced at higher doses is higher but with a smaller dose dependence, indicating saturation. The saturation level is comparable but higher for SS316L than for SS304L, indicating a stronger hardening for the first steel. Although saturation seems to start at about 1 dpa, there are not sufficient measurements at dose levels where the possible transition occurs to really establish it. But, if a comparison is made with other values in the literature obtained under approximately the same experimental conditions, the trends can be clearly shown. Values found in the literature are plotted in Fig. 2, where, for reasons of clarity, results for SS304 (a) and SS316 (b) are plotted separately, including the results from the present investigation. Although the scatter of the results is important (coming from differences in materials and irradiation conditions), the trend indicates clearly that a transition to a lower hardening rate takes place in the region of 1–3 dpa in both steels.

Comparing the results obtained in room temperature testing with those at 550 K, it can be seen that while SS316 shows no particular temperature effects, SS304 hardens more at higher temperature. This behaviour is discussed below in terms of deformation modes.

### 3.3. Deformation microstructure

Following the tensile tests, TEM investigations were performed, in order to identify the deformation modes operating at different temperatures.

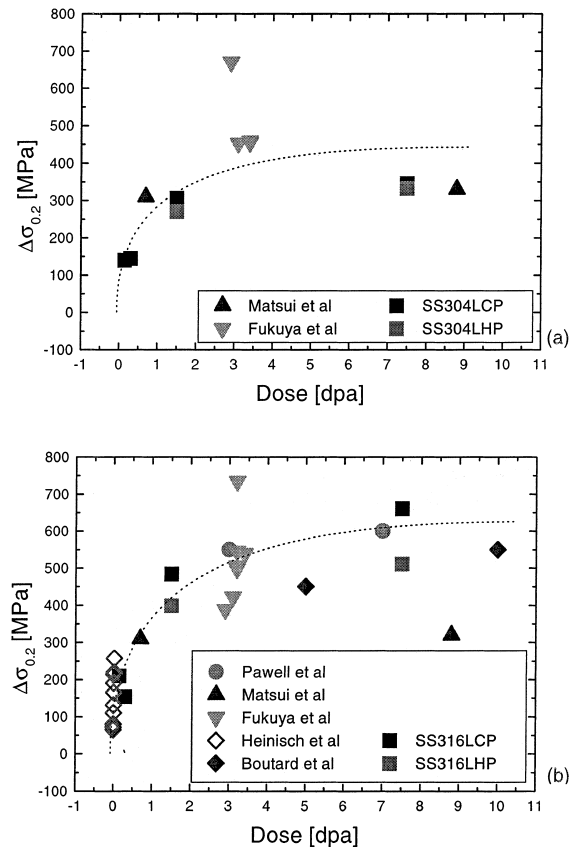


Fig. 2. Increase in yield strength as a function of dose for: (a) SS304; (b) SS316, comparison between our results and the literature [7–13].

Both steels show deformation twinning as a mode of deformation at low doses. The microtwins are very narrow (30 nm) and free of defects. Microtwins were determined using diffraction patterns. At room temperature, with increasing dose, no transition to another mode of deformation was found. However, at 550 K, while SS316 still deforms by twinning, SS304 shows channelling as mode of deformation at 1.5 dpa. The deformation channel density is qualitatively smaller to the microtwin density. The strain released at grain boundaries seems to be important in both cases. However, the high density of microtwins seems to accommodate more easily the strain. Fig. 3 shows the intersection of an annealing twin with deformation microtwins in a sample of SS316, tensile tested at 550 K up to necking. SS304 tested under the same experimental conditions is shown in Fig. 4, which shows the intersection between two channels and a grain boundary. The first intersection, the upper one, occurs when a channel appears to go through the grain boundary. The second channel does not travel through the grain boundary. In both cases, an important strain field is clearly visible on



Fig. 3. HP SS316 L, tensile tested at 550 K up to necking. The neutron irradiation dose is 1.5 dpa. Bright field picture shows intersections of different types of twins.

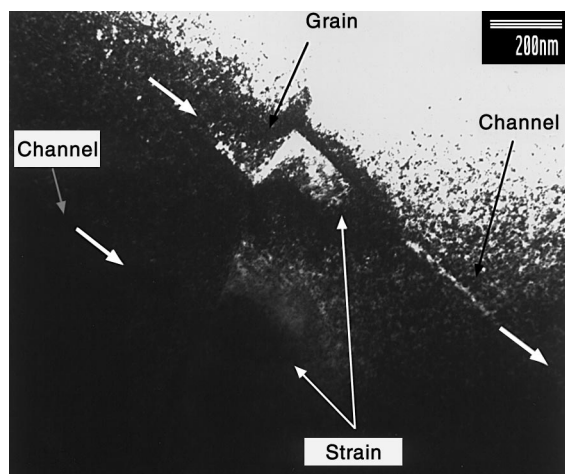


Fig. 4. HP SS304L, tensile tested at 550 K up to necking. The neutron irradiation dose reached 1.5 dpa. The bright field picture shows the intersection between a grain boundary and two dislocation channels.

the micrograph. In the second case, the strain field induced by the dislocation pile-up has probably not reached the critical value in order to nucleate a channel in the adjacent grain.

### 3.4. Deformation modes and hardening

TEM investigation revealed two different deformation modes: twinning and channelling.

In the twinning or channelling modes of deformation, the increase in yield strength is controlled by the glide of dislocations and their interaction with the irradiation defects. A first point to make from the present observations is that both channels and microtwins are free from irradiation-induced loops, which implies that in both cases the interaction of moving dislocations with the loop obstacles leads to their annihilation. This is the well-known mechanism of the formation of channels, but it is shown here that it also applies to the formation of deformation microtwins. Both deformation modes will induce a strong strain localisation at grain boundaries and therefore increase the cracking susceptibility as previously measured using SEM [3].

When material is deformed by channelling, the hardening induced by the irradiation defects was found to be higher than when twinning operated. Because twinning is a unidirectional process [14], the decrease in number density of the defects on the glide plane should be faster than in the case of channelling. Therefore, the dislocations will encounter less resistance and less hardening should take place.

### 3.5. Correlation with IASCC results

Results of an investigation using constant extension rate tests (CERT) on the same stainless steels conducted by ABB Sweden showed that SS316 samples were much less susceptible to IASCC than SS304 [15,16]. The specimens were strained at a rate of approximately  $10^{-8} \text{ s}^{-1}$ . The constant stress levels applied were chosen to correspond approximately to 50% and 100% of the yield strength in the unirradiated condition at 550 K. Although the material composition seems to be a key parameter, no clear reason was given why SS316 was less susceptible.

In comparison with the present study, the higher sensitivity at 550 K to IASCC can be explained by the more localised deformation mode taking place in SS304L than in SS316L. The dislocation channelling mode of deformation will induce localised plasticity leading to failure. The hardening by itself seems not to be a good criterion for IASCC susceptibility, but rather the deformation mode should be considered.

## 4. Conclusion

In the present work, the effects of irradiation on austenitic stainless steels have been investigated. The tensile properties, microstructure and deformation modes have been detailed.

The irradiation hardening increases linearly to a saturation level. The saturation level is higher for SS316L than for SS304L and takes place around 1 dpa.

The hardening levels and saturation are in good agreement with those found in the literature.

The mean loop size at 0.15 dpa is about 2.5 nm and with increasing irradiation dose, the mean loop size increases to approximately 8 nm. SS316L shows systematically lower densities and smaller mean defect size than SS304. The density and the average defect size increases with dose. The loop density is between  $1.2 \times 10^{23} \text{ m}^{-3}$  at 0.15 dpa and  $3 \times 10^{23} \text{ m}^{-3}$  for SS304L and between  $1.7 \times 10^{22}$  and  $1.8 \times 10^{23} \text{ m}^{-3}$  for SS316L. The density increases with dose and this increase is larger for SS316L than SS304L.

Both SS304L and SS316L show twinning as a mode of deformation. The microtwins are very narrow and free of defects. At room temperature, no transition to another deformation mode produced by irradiation was found. However, at 1.5 dpa, HP SS304L, tensile tested at 550K, showed dislocation channelling. At 550K, the deformation mechanism of SS316L is still twinning, like at room temperature. The stress released at the grain boundaries seems to be important in both cases. Both channels and microtwins are highly localised, defect free and deformation modes that will induce microcracking at grain boundaries and could lead to failure.

Radiation hardening by itself seems not to be a good criterion for IASCC susceptibility, but rather the deformation mode should be considered. The low resistance to IASCC of SS304L can be explained by dislocation channelling mode of deformation, inducing a highly localised deformation.

#### Acknowledgements

The financial assistance of ABB Sweden is gratefully acknowledged.

#### References

- [1] G.S. Was, S.M. Bruemmer, *J. Nucl. Mater.* 216 (1994) 326.
- [2] P.L. Andresen, F.P. Ford, S.M. Murphy, J.M. Perks, in: *Stress Corrosion Cracking – Material Performance and Evaluation*, ASM, Materials Park, Vol. 6, 1992, p. 91.
- [3] C. Bailat, F. Gröschel, M. Victoria, *J. Nucl. Mater.* 276 (1999) 283.
- [4] P. Marmy, M. Daum, D. Gavillet, S. Green, W.V. Green, F. Hegedus, S. Proennecke, U. Rohrer, U. Stiefel, M. Victoria, *Nucl. Instrum. and Meth. B* 47 (1990) 37.
- [5] Y. Dai, M. Victoria, *Microstructure Evolution During Irradiation*, Materials Research Society, Pittsburgh, PA, 1996.
- [6] D. Tabor, *J. Inst. Met.* 20 (1951) 79.
- [7] J.E. Pawel, A.F. Rowcliffe, D.J. Alexander, M.L. Grosbeck, K. Shiba, *J. Nucl. Mater.* 233 (1996) 202.
- [8] J.E. Pawel, A.F. Rowcliffe, G.E. Lucas, S.J. Zinkle, *J. Nucl. Mater.* 239 (1996) 126.
- [9] Y. Matsui, M. Niimi, T. Hoshiya, F. Sakurai, S. Jitsukawa, T. Tsukada, M. Ohmi, äH. Sakai, R. Oyamada, T. Onchi, *J. Nucl. Mater.* 233 (1996) 188.
- [10] K. Fukuya, S. Shima, K. Nakata, S. Kasahara, A.J. Jacobs, G.P. Wozadlo, S. Susuki, M. Kitamura, in: R.E. Gold, E.P. Simonen (Eds.), *Sixth International Symposium on Environmental Degradation of Materials in Nuclear Power System – Water Reactor*, Minerals, Metals and Materials Society, Vol. 565, 1993.
- [11] H. Heinisch, M.L. Hamilton, W.F. Sommer, P.D. Ferguson, *J. Nucl. Mater.* 191 (1992) 1177.
- [12] G.R. Odette, G.E. Lucas, *J. Nucl. Mater.* 179 (1991) 572.
- [13] J.L. Boutard, *J. Nucl. Mater.* 174 (1990) 240.
- [14] A.S. Argon, in: R.W. Cahn, P. Haasen (Eds.), *Physical Metallurgy*, 4th Ed., Vol. 3, 1996.
- [15] A. Jenssen, L.G. Ljungberg, *Minerals*, in: *Sixth International Symposium on Environmental Degradation of Materials in Nuclear Power System – Water Reactor*, Minerals, Metals and Materials Society, Vol. 547, 1993.
- [16] A. Jenssen, L.G. Ljungberg, in: *Seventh International Symposium on Environmental Degradation of Materials in Nuclear Power System – Water Reactor*, Breckenridge, 1995, p. 1043.